Electron-Beam Micrometallurgy: High-Chromium Steels[1]

Yu.F. Ivanov

Institute of High Current Electronics, 2/3 Akademichesky ave., Tomsk, 634055, Russia,
Tel.+7-3822-491713, Fax +7-3822-492-410, E-mail: yufi@mail2000.ru

Abstract – By TEM method carried out investigations of industrial steels of austenitic and ferritic classes, treated by electron beam. It was revealed a possibility of formation in the surface layer of steel containing submicron inclusions of the second phase particles, structure and phase composition characteristic for high-alloyed materials.

1. Introduction

The successes in the field of physics of high densities energy generation (pulse laser, electron and ion beams, plasma flows) lead to development of steel modification new methods, based on application of concentrated energy flows. The characteristic feature of concentrated energy flows impact is ultrahigh (10^8–10^{10} K/s) heating and cooling speeds, small (10^{-6}–10^{-3} s) times of high temperatures impact, small thickness layer of high densities energy concentration. Using of concentrated energy flows as modification way is accompanied increase of corrosion resistance, wearing capacity and microhardness of steel surface layers [1–3].

Work aim – laws exposure of electron-beam modification of high-chromium steel which has carbide phase submicron particles.

2. Experimental Procedure

As investigation material we used AISI 440A steel (0,65C–16,64Cr–0,4Mn–0,08Mo–0,36Si). Samples having cylindricity form (thickness of 10 mm and diameter of 20 mm) were treated by low energy high current electron beam (LEHCEB) with microsecond pulse duration. The parameters of LEHCEB were as follows: E_S=2,7–27 J/cm^2, τ=2,5 μs in single-pulse regime [4]. Steel melting threshold (smooth relief of irradiation surface, occurrence of weakly etching layer on occurrence section) was achieved at E_S~2,7 J/cm^2. At increase of energy beam density the thickness of white layer increased at E_S=27 J/cm^2 and was ~6 μm. Investigations of steel surface layer phase composition and defective substructure were carried out by methods of electron diffraction microscopy of thin foils.

3. Results and Discussion

According to data of TEM method, 440A steel in initial condition had a polycrystalline construction. Ferrite grains (solid solution of chrome and carbon in b.c.c. crystal lattice based on iron) with average size of ~15 μm contained network dislocation substructure with dislocation scalar density of $\langle\rho\rangle$ ~$2\cdot10^{10}$ cm^{-2}. Inside and along boundaries of grains globular particles of $M_{23}C_6$ ($(Fe,Cr)_{23}C_6$) type carbide were located. Carbide phase particles were monocrystals and practically had not dislocation substructure. Particles located in α-phase grains volume had a spherical form and average sizes of ~0,3 μm. Particles located along grains boundaries had ellipsoidal form and sizes of 0,5–1 μm. Particles located in grain boundary junctions had some volume belonging to contacting grains and that is why had not a definite form, their sizes were 0,8–1 μm. Volume fraction of carbide phase particles was ~0,2 of steel volume; distance between particles was ~2–2,5 μm.

At steel treatment by electron beam with energy density corresponding to initial melting stage (E_S~2,7 J/cm^2), $M_{23}C_6$ carbide globules under high temperatures and stresses are broken into weakly disorientated fragments (clusters) (Fig. 1, *a*, *b*). Electron diffraction pattern obtained from such particles have a big number of reflections not belonging to $M_{23}C_6$ crystal lattice. Therefore initially single-phase particles turn into multiphase aggregate (Fig. 1, *c*). Electron diffraction pattern interpretation allowed making a conclusion that the most probable phases are: C_2FeO_4, Cr_3C_2 and $M_{23}C_6$. Thus on the stage of thermal influence the process of carbide particle dissolution is carried out by carbon atoms outlet from globule volume with following formation of iron oxicarbide film around it. Particle decarbonization leads to chromium carbide formation of M_3C_2 [$(FeCr)_3C_2$] composition, i.e. phase differing from initial in carbon content. As a result of electron beam influence the average sizes of $M_{23}C_6$ carbide particles practically were not changed. It is possible to suppose that this transformation is carried out on the mechanism like "in situ" mechanism characteristic for carbide tran-

[1] The work was supported by RFBR grant (project №05-02-39008)

sformations in chromium steels. In this case dissolution reaction of carbide particle can be written down in the following way:

$$M_{23}C_6 \xrightarrow{C} M_{23}C_6+(FeCr)_3C_2+C_2FeO_4.$$

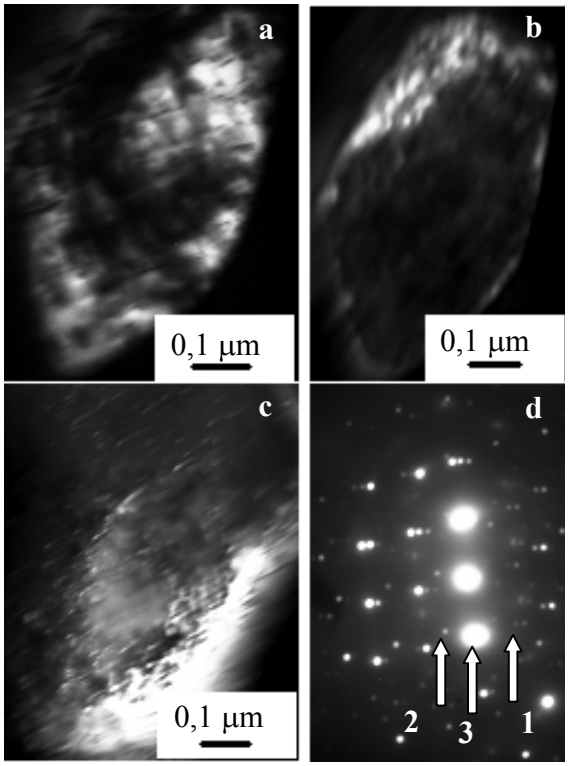

Fig. 1. Substructure of $M_{23}C_6$ globular carbide. LEHCEB (2,7 J/cm^2; 2,5 μs); a–c – TEM dark-field images, obtained in reflections [331]$M_{23}C_6$, [224]$M_{23}C_6$, [115] $M_{23}C_6$ + [110] α-Fe, correspondingly; d – diffraction pattern, obtained from these particle. Dark-field reflections are marked by figures: 1 – (a), 2 – (b), 3 – (c).

Carbon outlet from carbide particle leads to formation of oversaturated solid solution. Following high-speed hardening is accompanied by its decay with formation of volume surrounding globule with a thickness of ~200 nm of the second phase nanosize particles (Fig. 1, *c*). Chrome carbides can be such phase. Really from thermal calculations it is follows that in analized case T_{max}~2000 K, and melt thickness is ~0,5 μm. As long as for carbide $Cr_{23}C_6$ T_m=1845 K, during α-matrix (~10^{-6} s) melt lifetime surface liquid-phase dissolution of initial carbide particles take place. Taking diffusion coefficient of chrome atoms in iron melt as D~10^{-4} cm^2/s, we will obtain that characteristic diffusion length of these atoms in liquid phase is ~100 nm.

Dissolution of particles located along -phase grains boundaries are accompanied by formation of lengthy layers (Fig. 2). Microdiffraction analysis (Fig. 2, *c*, *d*) showed that the layers are formed by particles of chrome carbide of type $Cr_{23}C_6$ and Cr_3C_2. Obviously, these particles formation is caused by grain boundary diffusion of chrome and carbon atoms in process of globule dissolution at steel heating with their following release at cooling in form of carbide phase particles.

Thus on the stage of flash (E_S~2,7 J/cm^2) dissolution of chrome carbide particles is carried out by carbon and chrome output from the volume occupied by the particle. At that particle average sizes practically are not changed.

At values of energy density LEHCEB of $E_S \geq 5$ J/cm^2 in steel layer hardened from the liquid state the structure characteristic for melt cellular crystallization is formed [5]. Increase of electron beam energy density influences this structure volume fraction. At E_S=5 J/cm^2 cellular structure take just near-boundary volume, dividing α-phase and carbide particle (Fig. 3), at E_S~27 J/cm^2 – cellular structure covers the most part of grain volume.

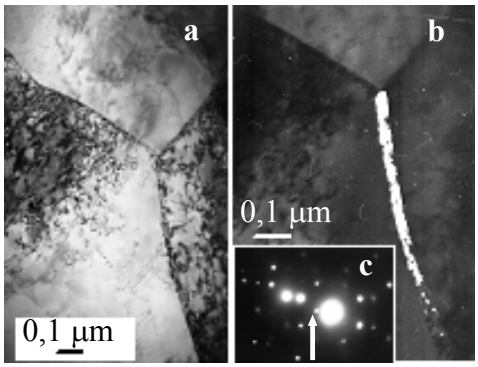

Fig. 2. Surface layer structure of AISI 440A steel treated by LEHCEB (2,7 J/cm^2, 2,5 μs); a – TEM bright field image; b – TEM dark field image, obtained in reflection [002]$M_{23}C_6$, c – diffraction pattern (dark field reflection is marked by the arrow)

Independently on energy density magnitude (in investigated in paper range), cells are weakly disorientated, and have a round shape, their average sizes change in range of 70–80 nm (Fig. 3). Cells are defectless, dislocation substructure inside of cells is absent. Microdiffraction analysis of cellular structure with the following diffraction pattern interpretation showed that independently on E_S magnitude cells have b.c.c. lattice like α-phase lattice. Cells are divided by the second phase layers clearly identifiable by dark-field method (Fig. 4). At energy density of E_S~5 J/cm^2 layers are amorphous. Obtained from cellular structure diffraction pattern contents the point reflections of α-phase and diffusive rings (Fig. 3, *d*). Most likely layer amorphization is caused by increased concentration of carbon in the liquid phase (in initial particle that is ~20 at. %), also by high speed of melt cooling.

Increase of electron beam energy density up to ~18 J/cm^2 leads to practically full dissolution of $M_{23}C_6$ initial particles and following melt cellular crystallization with the formation in some cases layers with crystal structure along cells boundaries (Fig. 4, *c*, *d*). The change of diffraction pattern-dif-

fuse halo is broken into separately located point reflections shows it (Fig. 4, *d*).

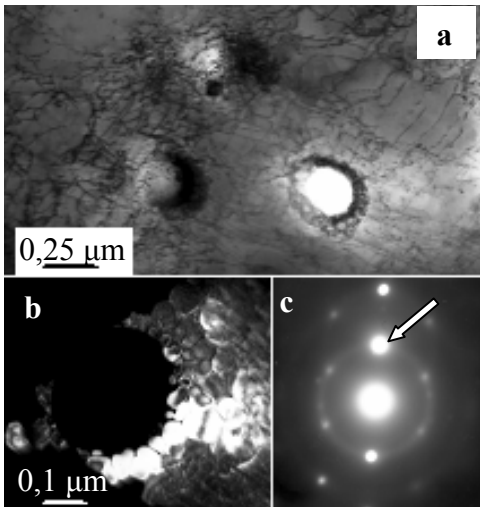

Fig. 3. Surface layer structure of AISI 440A steel treated by LEHCEB (5,7 J/cm^2, 2,5 μs). a – TEM bright field image; b – TEM dark field image, obtained in reflection [110] α-Fe, c – diffraction pattern, containing point reflections of crystal phase and diffusive rings belonging to amorphous phase (dark field reflection is marked by the arrow)

It should be mentioned, that at diffraction pattern interpretation we considered a possibility of chrome and iron carbides formation. The last one is stipulated by the iron carbide particles formation is related mainly to carbon atoms diffusion, and consequently at small times of thermal influence the possibility of their output is more preferable in comparing with chrome carbides.

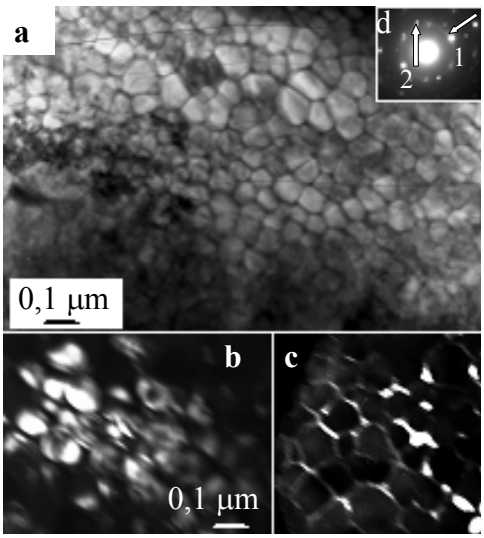

Fig. 4. Structure of surface layer crystallization of AISI 440A steel treated by LEHCEB (27 J/cm^2, 2,5 μs); a – TEM bright field image; б, c – TEM dark field images, obtained in reflections [110]α-Fe (b), [111]Cr_3C_2 (c); d – diffraction pattern, dark field reflection is marked by the arrows: 1 – (b), 2 – (c)

The comparative analysis of interpretation results of diffraction pattern given on Fig. 4, *d* showed that the iron carbide of $Fe_{20}C_9$ composition has the closest to experimentally measured combination of radius-vectors R(hkl).

Steel treatment by electron beam in visible evaporation regime (~27 J/cm^2) leads to structure formation where crystallization cells cover the most part of surface layer (Fig. 5). The second phase located along cells boundaries is in crystal state. Obviously that is related to decrease of hardening speed (increase of melt temperature) to increase of electron beam energy density. Decrease of hardening speed contributes also to coagulation of the second phase dividing cells. The last one leads to gradual cells degradation and formation of structure consisting of nanosize carbide particles chaotically located in ferritic matrix (Fig. 5, *a*).

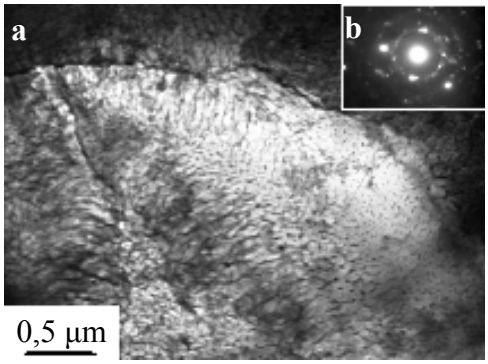

Fig. 5. Structure of surface layer crystallization of AISI 440 A steel treated by LEHCEB (27 J/cm^2, 2,5 μs); a – TEM bright field image; b – diffraction pattern of (a)

Interpretation of diffraction pattern given on Fig. 5, *b*, showed that outstanding phase is chrome carbide of Cr_3C_2 composition. Formation of chrome carbide (but not iron carbide) can be caused by as well increase of thermal influence time as by possible changing of steel surface layer chemical composition.

Surface layer concentration by chrome at E_s=16 J/cm^2 can be explained in the next way. In irradiation results this layer is carbonized from vacuum chamber latent atmosphere. Due to chrome has larger sensitivity to carbon than iron has (chrome is stronger carbide former), there is a diffusion of chrome atoms from target depth to carbonized surface. Obviously at pulse treatment such chrome atoms redistribution in steel is possible just in conditions of melt existence. Really taking into account that at heating in solid phase (1350 °C) diffusion coefficient of chrome atoms in iron is D~5·10^{-8} cm^2/s [6], and duration of high-temperature stage t~10^{-5} c (high estimation), we will obtain that diffusion length of chrome atoms range in iron is ℓ~$(D \cdot t)^{1/2}$~10 nm. This magnitude is less considerably than thickness of layer where chrome redistribution is observed. In case of liquid-phase of chrome atoms diffusion in iron

(D~10^{-4} cm^2/s) we will obtain that within melt existence time(t_m~$7 \cdot 10^{-6}$ s) magnitude is ℓ~0,26 μm [6].

4. Conclusions

Thus, LEHCEB irradiation of AISI 440A high-chromium steel leads to two variants behavior of conversion of submicron size $M_{23}C_6$ carbide globules contained in initial state. At small values of electron beam energy density (~2,7 J/cm^2), corresponding steel melting initial stage (stage of surface relief smoothing), it is observed particles conversion under "on the spot" mechanism. In this case as a result of primary output of carbon atoms from the volume covered by particle inside of it we observe formation of chrome carbide particles of Cr_3C_2 composition. Liquid-phase particle dissolution by output from surface to grain volume of α-phase carbon and chrome atoms leads to formation of nano-size chrome carbide particles and around the globule, grain boundary diffusion of chrome atoms contributes to formation of carbide phase lengthy layers along α-phase grain boundaries.

At high values of electron beam energy density (the stage of steady melting) liquid-phase globule dissolution leads to melt cellular crystallization with formation of α-phase nano-size cells divided by layers of amorphous or crystal (depending on treatment temperature-time parameters) phases. Layers crystallization carries with formation of carbide phases based on iron and chrome.

References

[1] V.A. Gribkov, F.I. Grigoriev, B.A. Kalin, V.L. Yakushin. *Perspektivnye radiacionno-puchkovye tehnologii obrabotki materialov*, Moscow, The whole year round, 2001, 528 pp.

[2] V.D. Sadovskii, V.M. Schastlivsev, T.Ya. Tabatchikova, I.L. Yakovleva, *Laser heating and steel structurei*, Sverdlovsk, UB, USSR AS, 1989, p. 101.

[3] V.S.Kraposhin, Itogi Nauki i Tekh., Moscow, VINITI 21, 144 (1987).

[4] E.M.Oks, P.M.Schanin, Pribory i Tekhnika Experimenta 3, 166 (1988).

[5] *Surface modification and allowing by laser, ion and electron beams,* Ed. by J. Poate, G. Foti and D(G). Jacobson, Moscow, Mashinostroenie, 1987, 424 pp.

[6] A.P. Babichev, N.A. Babushkin, A.M. Bratkovskij et al. *Fizicheskie velichiny. Spravochnik*, Moscow, Energoatomizdat, 1991, 1232 p.